



RESEARCH LETTER

10.1029/2017GL076246

Key Points:

- Satellite observations and an eddy-rich model show positively/negatively correlated anomalies of sea level and chlorophyll in summer/winter
- In summer, higher/lower iron concentration in positive/negative sea level anomalies leads to higher/lower chlorophyll
- In winter, deeper/shallower mixed layers in positive/negative sea-level anomalies decrease/increase chlorophyll through light limitation

Supporting Information:

- Supporting Information S1

Correspondence to:

H. Song,
hajsong@mit.edu

Citation:

Song, H., Long, M. C., Gaube, P., Frenger, I., Marshall, J., & McGillicuddy, D. J. Jr. (2018). Seasonal variation in the correlation between anomalies of sea level and chlorophyll in the Antarctic Circumpolar Current. *Geophysical Research Letters*, 45. <https://doi.org/10.1029/2017GL076246>

Received 31 OCT 2017

Accepted 12 MAY 2018

Accepted article online 17 MAY 2018

Seasonal Variation in the Correlation Between Anomalies of Sea Level and Chlorophyll in the Antarctic Circumpolar Current

Hajoon Song¹ , Matthew C. Long² , Peter Gaube³ , Ivy Frenger⁴ , John Marshall⁵ , and Dennis J. McGillicuddy Jr.⁶ 

¹Department of Atmospheric Sciences, Yonsei University, Seoul, Korea, ²Climate and Global Dynamics Laboratory, National Center for Atmospheric Research, Boulder, CO, USA, ³Applied Physics Laboratory, University of Washington, Seattle, WA, USA, ⁴GEOMAR Helmholtz Center for Ocean Research Kiel, Kiel, Germany, ⁵Department of Earth, Atmospheric and Planetary Sciences, Massachusetts Institute of Technology, Cambridge, MA, USA, ⁶Department of Applied Ocean Physics and Engineering, Woods Hole Oceanographic Institution, Falmouth, MA, USA

Abstract The Antarctic Circumpolar Current has highly energetic mesoscale phenomena, but their impacts on phytoplankton biomass, productivity, and biogeochemical cycling are not understood well. We analyze satellite observations and an eddy-rich ocean model to show that they drive chlorophyll anomalies of opposite sign in winter versus summer. In winter, deeper mixed layers in positive sea surface height (SSH) anomalies reduce light availability, leading to anomalously low chlorophyll concentrations. In summer with abundant light, however, positive SSH anomalies show elevated chlorophyll concentration due to higher iron level, and an iron budget analysis reveals that anomalously strong vertical mixing enhances iron supply to the mixed layer. Features with negative SSH anomalies exhibit the opposite tendencies: higher chlorophyll concentration in winter and lower in summer. Our results suggest that mesoscale modulation of iron supply, light availability, and vertical mixing plays an important role in causing systematic variations in primary productivity over the seasonal cycle.

Plain Language Summary In the Southern Ocean, the Antarctic Circumpolar Current is characterized by highly energetic eddies with anomalous water mass properties such as sea level and temperature. We can also expect that eddies perturb biogeochemical conditions. From the satellite observations, we found that anticyclonic eddies with anomalously high sea level have elevated chlorophyll biomass while cyclonic eddies with a negative sea-level anomaly have less-than-average chlorophyll in summer. Strikingly, this relationship reverses in winter: lower chlorophyll in anticyclonic eddies and higher chlorophyll in cyclonic eddies. Using eddy-rich numerical model, we show that this seasonally changing relationship results from alternating limiting factor for the primary production. In summer, anticyclonic eddies have elevated iron that promotes primary production through enhanced vertical mixing. In winter, however, enhanced vertical mixing reduces the light level and prevents primary production. This study shows that the mesoscale eddies can perturb primary production by affecting two limiting factors (iron and light) alternatively.

1. Introduction

The ocean is rich in mesoscale phenomena that account for more than 90% of the kinetic energy in the surface ocean (Ferrari & Wunsch, 2009) and are known to play a critical role in transporting momentum, heat, and energy (Robinson, 1983; Wunsch, 1999; Xu et al., 2014). The mesoscale modulates marine ecosystems via effects on both the physical and chemical environment, influencing, for instance, nutrient supply, light levels, and the diversity of phytoplankton populations (Clayton et al., 2016; McGillicuddy et al., 2007; Rodríguez et al., 2001). This modulation is clearly seen in chlorophyll concentrations (CHL). Anomalies of satellite CHL, a proxy for phytoplankton biomass, are observed to be correlated with sea surface height (SSH) anomalies, a proxy for mesoscale phenomena, in many regions of the ocean (Chelton, Gaube, et al., 2011; Gaube et al., 2014). Depending on the prevailing mechanisms, both positive and negative correlations between SSH

and CHL ($\rho_{SSH,CHL}$) can be expected. A wide range of mechanisms have been proposed by which the mesoscale modulates biogeochemistry, as reviewed in McGillicuddy (2016).

In situ and satellite observations have revealed mixed-layer depth (MLD) modulation by mesoscale dynamics; deeper (shallower) MLDs are associated with anticyclones (cyclones) with positive (negative) SSH anomalies in the subtropical ocean (Dufois et al., 2014; Gaube et al., 2013) and also in the Southern Ocean (SO; Hausmann et al., 2017). While the influence of mesoscale dynamics on the MLD, nitrate, and CHL in the subtropical gyres has received some attention (Dufois et al., 2014, 2016), these processes remain understudied in the SO, which is a region of major importance for biogeochemical cycling and air-sea carbon exchange.

In much of the SO, the supply of iron and availability of light are key mediators of primary productivity (Boyd, 2002; Fauchereau et al., 2011). During summer when sunlight is abundant, primary productivity is mainly limited by iron, which is depleted in the surface ocean and enriched at depth (Boyd & Ellwood, 2010; Venables & Moore, 2010). In such conditions, introduction of iron-rich subsurface water through vertical mixing can enhance the primary productivity and increase CHL (Carranza & Gille, 2015). In contrast, during the winter, deep convective mixing supplies iron to the upper ocean (Tagliabue et al., 2014) but simultaneously decreases mixed-layer-average light levels for photosynthesis (Nelson & Smith, 1991). Fauchereau et al. (2011) found large spatial and seasonal variability in the correlation between CHL and MLD and proposed vertical mixing as an important driver for the surface CHL perturbation through changes in limitation by either iron or light.

If the mesoscale modulation of MLD has a significant impact, we can anticipate that deeper vertical mixing in anticyclones would supply iron-rich subsurface water more than cyclones in summer but decreases light level further in winter when compared with cyclones. Then the footprint of mesoscale modulation of MLD on CHL would appear as a seasonal cycle in $\rho_{SSH,CHL}$. This raises the question, do satellite observations of SSH and CHL reveal such a signal? In this study, motivated by the systematic modulation of MLD by the mesoscale and its link to factors limiting productivity, we examine $\rho_{SSH,CHL}$ at the mesoscale in the SO where the mean eddy scale is between 75 to 100 km (Chelton, Schlax, et al., 2011). We utilize satellite observations and an eddy-rich biogeochemical numerical model to better understand the physical and biological interactions in the mesoscale.

After briefly describing the observations and physical-biogeochemical model, we first report on observed $\rho_{SSH,CHL}$ in the SO, particularly along the Antarctic Circumpolar Current (ACC). We then evaluate the influences of MLD modulation by mesoscale dynamics on the observed correlation by utilizing a numerical model.

2. Satellite Data and an Eddy-Rich Physical-Biogeochemical Model

The procedure to obtain the anomaly of SSH and CHL starts from preparing weekly mean fields from 1998 to 2007. The weekly mean SSH field was prepared by averaging the daily absolute dynamic topography mapped on the $0.25^\circ \times 0.25^\circ$ degree grid by Collecte Localis Satellites/Archiving, Validation and Interpretation of Satellite Oceanographic data (CLS/AVISO). This data set does not contain mesoscale variability whose length scale is smaller than 0.4° (Chelton, Schlax, et al., 2011). The processes to obtain the weekly CHL include mapping log-transformed daily CHL estimation from Sea-Viewing Wide Field-of-View Sensor (SeaWiFS) on the same grid as SSH anomalies, applying loess smoother in time and transforming back to its original linear scale (Gaube et al., 2013). The weekly average attenuates the features whose time scale is shorter than a few days (e.g., submesoscale features). Then the anomalies of SSH and CHL were estimated by spatially high-pass filtering the weekly data with 6° half-power cutoff, which retains the variability with wavelength scale shorter than 6° . Details of the processing are provided in the supporting information.

We evaluate the role of mesoscale phenomena by considering SSH anomalies exceeding 5 cm in absolute value. Such deviations in SSH include those driven by not only coherent eddy structures expressed by closed contours of anomalies (Chelton, Schlax, et al., 2011) but also other mesoscale flow features (e.g., fronts). Positive SSH anomalies represent anticyclones, while negative anomalies correspond to cyclones for coherent eddy structures. In case of fronts, a positive/negative SSH anomaly is likely to be found on the less/more dense side of the front in the SO where the sea level increases toward the equator. When identified from a few weekly maps of SSH anomaly using the same eddy detection algorithm as the one in Chelton, Schlax, et al. (2011), coherent eddy structures account for approximately 67% of SSH anomalies with the size greater than 5 cm. For simplicity, positive/negative SSH anomalies are referred to anticyclones/cyclones in this study, recognizing that the underlying phenomenology is more complicated.

A simulation of eddy-rich coupled physical and biogeochemical states is provided by a Biogeochemical Elemental Cycling model (Moore et al., 2002, 2004, 2013) embedded in the 0.1 resolution ocean circulation component of the Community Earth System Model. Phytoplankton growth is regulated by both light and nutrients (iron in this regime) as described in equation (S1). Vertical mixing is represented by the K-profile parameterization scheme (Large et al., 1994), in which diapycnal diffusivity is set proportional to the vertical mixing depth. We use the vertical mixing depth as a measure of MLD because the vertical mixing of tracers such as nutrients is subject to it. Although the vertical mixing depth is generally shallower than the MLD determined by potential density criteria in the model simulation, they show a strong correlation (correlation coefficient >0.8 with p value < 0.01). Hence, it is reasonable to expect that the vertical mixing depth (or MLD hereafter) is modulated by the mesoscale in a manner similar to that of the MLD. A detailed description of the model can be found in the supporting information.

3. Seasonal Correlation Between Anomalies of SSH and Chlorophyll

Our analysis of satellite observations of CHL and SSH anomalies reveals a positive $\rho_{SSH',CHL'}$ along the ACC in summer (January–March, Figure 1a) and a negative $\rho_{SSH',CHL'}$ in winter (July–September, Figure 1b; e.g., Frenger, 2013). In winter, the signal is not as clear as in the summer, which may be due to the lower CHL variability. The condition of low sun elevation, sun glint, and frequent storm system passages lowers the observational density of satellite CHL data in winter. Lower density can be problematic in computing the anomalies with respect to the spatial mean and possibly obscure the correlation signal. The seasonality of the correlation along the ACC is clearly different from that to the north of it where the correlation is generally negative all year long.

To identify the mechanisms by which mesoscale processes in the ACC influence CHL, we examine the solution of an eddy-rich physical-biogeochemical model. The 5-day mean model fields are first mapped on the same 0.25 grid as the satellite data using bilinear interpolation to suppress the impact from features that the satellite observations cannot represent. Encouragingly, the simulation largely reproduces the observed seasonality in $\rho_{SSH',CHL'}$ (Figures 1c and 1d), as well as SSH variability, mean, and seasonality of near-surface CHL and seasonal variability in the depth of mixed layer (Figures S1 and S2). There are broad areas of strongly positive $\rho_{SSH',CHL'}$ along the ACC and at its southern margins in summer, changing sign in winter, especially in the Indian and Pacific Ocean sectors. South of the ACC, correlations are noisier and observed and modeled correlations agree less, perhaps due to processes that are missing in the model, such as iron supply from melting sea ice, or possibly weaker observational constraints in the polar zone.

We examined $\rho_{SSH',CHL'}$ averaged zonally along the path of the ACC (defined by SSH isolines between -80 and -20 cm, see the supporting information) to draw out seasonal patterns. Correlations are positive within the ACC from summer to fall (January–June), then switch to negative until early spring (October; Figure 2a). Observations indicate that the seasonality in the correlation is lagged south of the regions with -50 cm SSH; the model, however, shows a more consistent phasing over the meridional extent of the ACC region (Figure 2b). In spite of this inconsistency, the simulation captures the major correlations in the ACC, justifying an examination of the simulation to identify the underlying mechanisms generating observed variability in mesoscale modulations of the CHL field.

4. Mechanisms in an Eddy-Rich Biogeochemical Model

We hypothesize that oceanic mesoscale dynamics play an important role in the seasonality of $\rho_{SSH',CHL'}$ along the ACC by regulating the availability of light and iron, resulting in differing CHL responses in summer and winter. There is a positive correlation between MLD and SSH anomalies in all seasons over most of the SO in the model, suggesting that anticyclones have deeper mixed layers than cyclones (Figures 1e, 1f, and 2e). This MLD modulation by the mesoscale is more intense and systematic in winter than in summer, evident in a larger MLD difference between anticyclones and cyclones (Figures 3a and 3b) and a higher correlation coefficient between anomalies of SSH and MLD (Figure 2e). The degree of mesoscale MLD modulation increases with the amplitude of the SSH anomaly. For example, the wintertime MLD difference between positive and negative SSH anomalies whose amplitudes are greater than 5 cm is 24 m; this statistically significant difference increases to 55 m when the amplitude of SSH anomalies greater than 20 cm are considered. The simulated correlation between SSH anomalies and MLD (Figure 2e), seasonality in mesoscale MLD modulation,

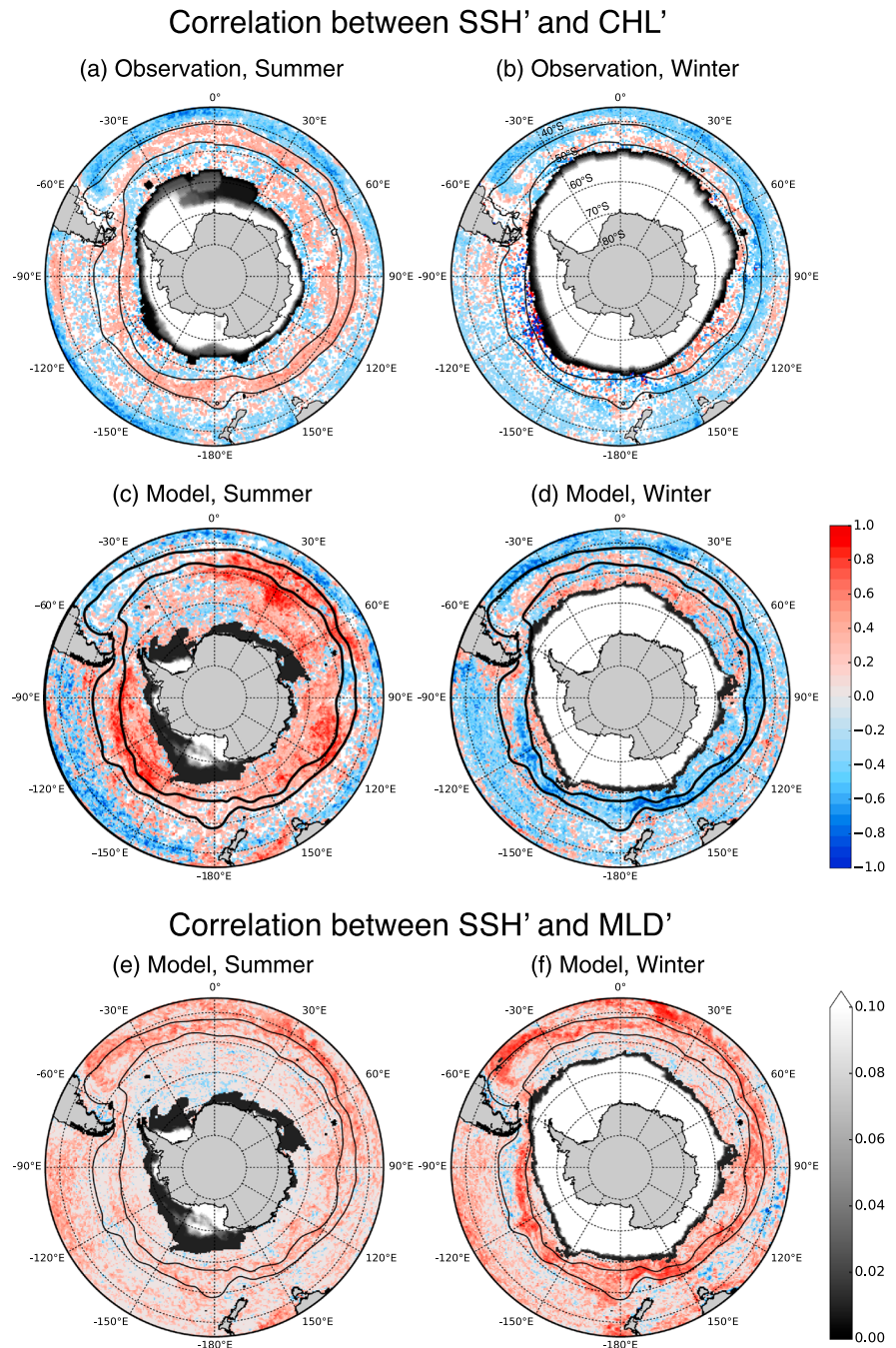


Figure 1. The correlation coefficients between anomalies of sea surface height (SSH) and chlorophyll concentration (CHL) in the (a and b) satellite observations and (c and d) 0.1 ocean model are shown as pseudo-color images. The left and right columns show the (a and c) correlation for austral summer (January–March) and (b and d) austral winter (July–September), respectively. Black contours mark the sea-level isolines of -20 and -80 cm that enclose the ACC. The masks in gray scale around Antarctica represent the sea-ice area fraction from the Hadley Centre Sea Ice and Sea Surface Temperature data set in (a) and (b) and from the model in (c) and (d). The sea-ice areas are masked by the color changing from white to black. The correlation coefficients between anomalies of SSH and MLD in the eddy-rich model are also presented similarly in (e) and (f). The areas in white have either a correlation coefficient close to zero or a p value greater than 0.01 (statistically insignificant).

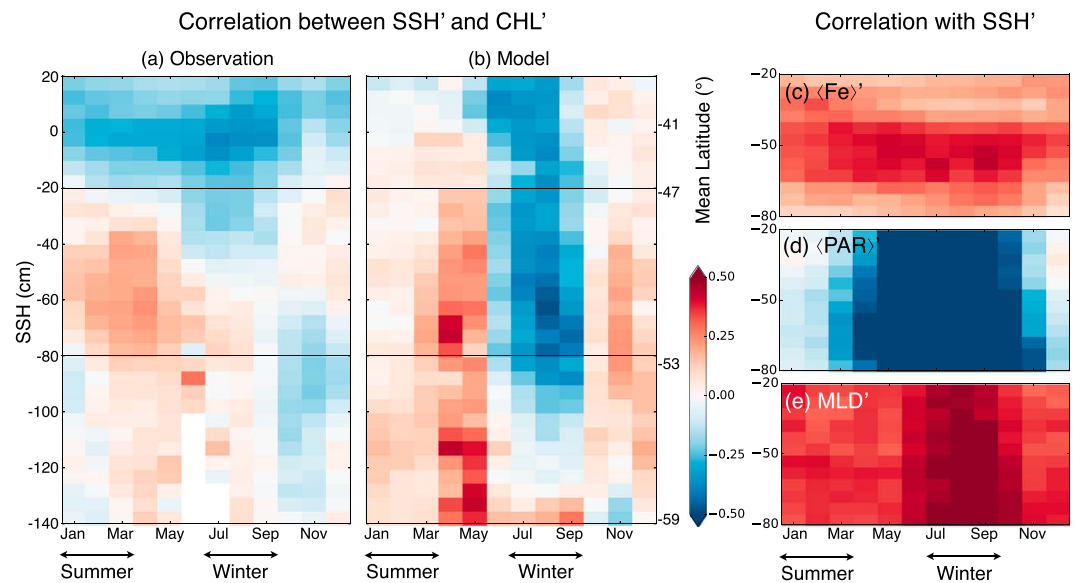


Figure 2. The correlation of anomalies in sea surface height (SSH) and chlorophyll concentration (CHL) along SSH isolines in (a) observations and (b) model. The areas within two black lines at -80 and -20 cm approximate the ACC and correspond to the black contours in Figure 1. The equivalent latitude is shown on the right y-axis in (b). Panels on the right are the correlation coefficients of anomalies of the (c) iron and (d) light limiting factor averaged over the mixed-layer depth (MLD), and (e) MLD with SSH anomalies from the model. Correlations are statistically significant at the 99% confidence level.

and dependency of MLD anomaly on the SSH anomaly amplitude are consistent with observed variations of MLD in eddies, whereby anticyclones exhibit weaker stratification and deeper mixed layers than cyclones (Hausmann et al., 2017).

In winter, light is the primary factor limiting productivity throughout the whole water column and iron limitation is of diminished importance (Figure 3b). Since light is supplied at the surface and attenuates with depth, simulated mixed-layer mean light (or photosynthetically active radiation; $\langle \text{PAR} \rangle$) declines with increasing MLD. We find that anomalies of $\langle \text{PAR} \rangle$ estimated from the model are negatively correlated with SSH anomalies throughout the year (Figure 2d). $\langle \text{PAR} \rangle$ is approximately 30% lower in anticyclones than cyclones in winter (Figure 4a) and about 7% lower in summer (Figure 4c), suggesting deeper mixing in anticyclones decreases $\langle \text{PAR} \rangle$ experienced by phytoplankton in the mixed layer. Thus, deeper vertical mixing in anticyclones has the potential to limit productivity in winter, resulting in lower CHL in anticyclones versus cyclones (Figures 3a and 3d). This argument is supported by the $\rho_{\text{SSH}, \text{CHL}}$ along the ACC in the Pacific and Indian Ocean sectors, although it is less clear in the Atlantic Ocean sector (Figures 1b and 1d). The Atlantic Ocean sector exhibits the shallowest mixed layers in winter that relieve the light limitation for the phytoplankton growth, leading to a less distinct relationship between anomalous vertical mixing and CHL. The Pacific and Indian Ocean sectors, however, have deeper mixed layers and clearer negative $\rho_{\text{SSH}, \text{CHL}}$ along the ACC in both the observations and the model than the Atlantic Ocean sector.

In contrast, productivity is iron limited in the summer (Figure 3a). The model simulation shows that anticyclones in the ACC have approximately 15% more iron averaged over the mixed layer ($\langle \text{Fe} \rangle$) in summer (Figure 4c) than cyclones, which promotes higher productivity and CHL. The $\langle \text{Fe} \rangle$ anomaly is larger in winter than in summer (30% versus 15%, Figures 4a and 4c), which suggests the link between the intensity of mesoscale MLD modulation and iron supply. However, the positive $\langle \text{Fe} \rangle$ anomaly associated with anticyclones in winter does not lead to enhanced productivity under the light-limited environment. Iron concentrations are elevated both within and below the mixed layer (Figures 3a–3c), suggesting that part of the enhanced vertical flux in anticyclones is attributable to a larger iron reservoir underlying these features at depth. Without anomalous deep mixing, the positive $\langle \text{Fe} \rangle$ anomaly in anticyclones cannot be maintained under the active consumption of iron by phytoplankton.

A budget analysis for $\langle \text{Fe} \rangle$ along the ACC (Figures 4b and 4d; see the supporting information for details) quantifies the various mechanisms of iron supply and removal. We only consider areas where bathymetry

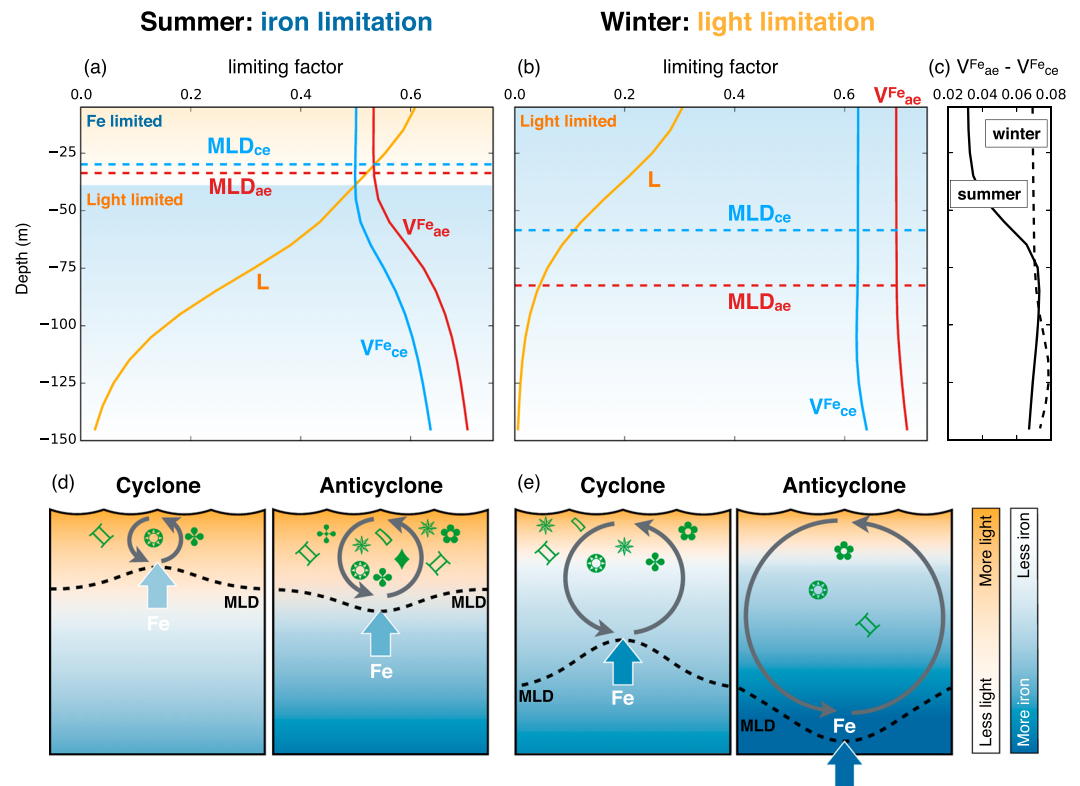


Figure 3. (a and b) The median vertical profiles of light limiting factor (L) and iron limiting factors ($V^{Fe} = Fe/(Fe + K_{Fe})$) for anticyclones (V^{Fe}_{ae}) and cyclones (V^{Fe}_{ce}) in the biogeochemical model (equation (S1)) averaged in the Antarctic Circumpolar Current (ACC). In summer, iron is the limiting factor for the primary productivity within the mixed layer (a). The magnitude of limiting factor is inversely related to its effect on primary productivity, for example, light is more important than iron concentration throughout the whole water column in winter (b). Blue and red dotted lines represent the median value for mixed-layer depth (MLD) within cyclones and anticyclones, respectively, in the ACC. Panel (c) displays the vertical profile of the iron limiting factor differences ($V^{Fe}_{ae} - V^{Fe}_{ce}$) in summer (solid line) and winter (dashed line). Confidence intervals of the MLDs are omitted in (a)–(c) because they are too narrow. A diagram depicting the mesoscale modulation of MLD and its impact on phytoplankton biomass in two different seasons in the Southern Ocean are shown in panels (d) and (e). The brightness of the blue and orange shading represents the iron concentration and sunlight intensity, respectively. In summer, primary production is controlled by iron supply (blue arrows) and not light in the mixed layer (d). In winter, intensive vertical mixing enriches iron concentration near the surface, but low light availability limits primary production (e).

is deeper than 200 m in order to avoid the direct influence from shelf regions (Carranza et al., 2017). Iron is supplied to the mixed layer by lateral and vertical advection, vertical mixing, aeolian input of dust, and entrainment associated with changes in the MLD; it is removed through the biogeochemical sink term, which represents phytoplankton uptake and scavenging on sinking particulates. Among these processes, we find that the supply of iron by vertical mixing differs most between anticyclones and cyclones. Supply of iron by vertical mixing in anticyclones has a median value that is roughly 10% higher than in cyclones when normalized by the median $\langle Fe \rangle$ in the ACC. The contributions from lateral and vertical advection tend to cancel each other, reducing the contribution as a whole, and the difference in median value of the total advection between anticyclones and cyclones is less than 1%. The differences in other terms are also small (less than 2%) compared to that in the vertical mixing. Iron input from dust increases $\langle Fe \rangle$ but, as might be expected, the differences between anticyclones and cyclones are negligible. The biogeochemical sink is the largest in summer with slightly more loss of iron in anticyclones due to higher phytoplankton productivity. The entrainment term shows little contribution after being normalized by the MLD, and differences between anticyclones and cyclones are negligible; thus, it is not plotted in Figures 4b and 4d.

Supply of iron through vertical mixing is controlled by both the MLD and the vertical gradient of iron, suggesting that knowing the vertical structure of iron is important to understand the enhanced vertical mixing term in anticyclones, especially in summer when the MLD differences between anticyclones and cyclones

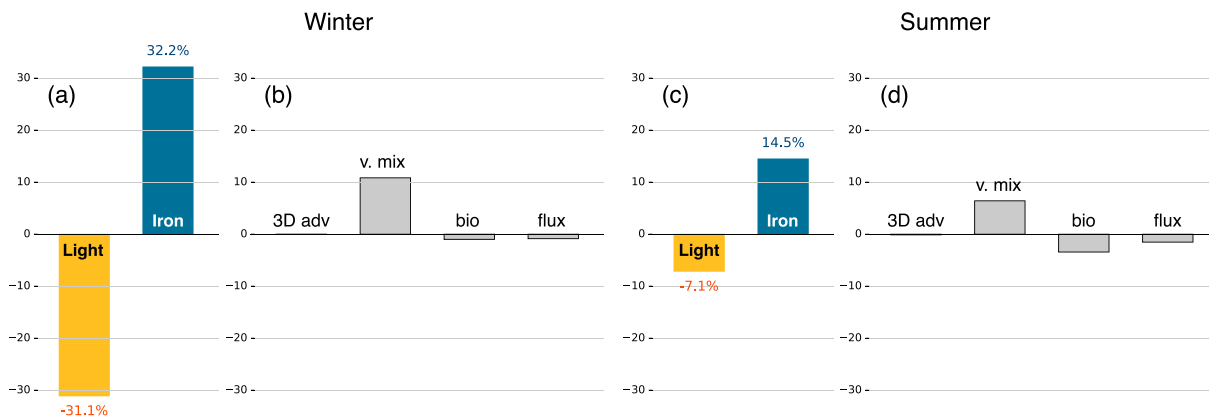


Figure 4. The bar plots in (a) and (c) represent the percentage differences in light level (yellow) and iron concentration (blue) in the mixed layer between anticyclones and cyclones in winter and summer, respectively. The percentage differences between anticyclones and cyclones in various contribution to the iron averaged over the mixed layer are plotted in (b) and (d). Those contributions are three-dimensional advection (3-D adv including both buoyancy- and wind-driven transports), vertical mixing (v. mix), biogeochemical cycle (bio), and flux from dust (flux), and they are normalized by the averaged iron in the mixed layer. The contribution from entrainment is little and not plotted. The 95% confidence intervals estimated using bootstrapping are narrow and not shown.

are relatively small. The model simulation suggests that anticyclones have an enhanced vertical iron gradient relative to cyclones in summer. The iron limiting factor shows a smaller difference between cyclones and anticyclones at the surface than at 50 m (the solid line in Figure 3c), suggesting that anticyclones have more favorable conditions for the enhanced iron supply by vertical mixing than cyclones. Combined with the fact that both the observations (Hausmann et al., 2017) and the model simulation (Figures 3a and 3b) suggest that MLD modulation by the mesoscale is relatively subtle in summer, the enhanced vertical iron gradient in anticyclones may be the key feature driving differences in iron supply by vertical mixing—as opposed to changes in the depth of mixed layer.

5. Discussion

Our study emphasizes the importance of mesoscale processes affecting phytoplankton growth through MLD changes impacting iron and light availability. Features with anomalously high SSH (anticyclones) are characterized by deeper mixed layers while those with negative SSH anomalies (cyclones) have anomalously shallow MLDs. These modulations of the MLD affect light levels resulting in lower CHL in anticyclones, and higher CHL in cyclones in winter. The MLD modulation by the mesoscale is also seen in summer, and the median MLD difference is statistically significant but small: less than 5 m along the ACC. Nevertheless, deeper MLDs and larger vertical gradients of iron together make iron supply by vertical mixing greater in anticyclones than cyclones and contribute to iron anomalies in the mixed layer in all seasons. Our results suggest that anomalies in iron availability and light exposure associated with the mesoscale and the alternating role of iron and light limitation in summer and winter play a major role in explaining the seasonally changing $\rho_{SSH,CHL}$ along the ACC (Figures 3e and 3f).

The eddy-rich biogeochemical model generates higher levels of iron in anticyclones along the ACC in both seasons. A possible explanation for higher iron in anticyclones in summer is preconditioning during winter. In winter when the MLD modulation by the mesoscale is particularly intense, deeper mixed layers in anticyclones have considerably higher iron concentration than the shallower mixed layers of cyclones. Anomalously high iron in anticyclones in winter is not heavily used due to the lack of sunlight and subsequently may promote elevated primary productivity in summer. The mixed layer shoals rapidly after winter, and iron in the mixed layer is consumed by primary producers, creating vertical gradients of iron. Then vertical mixing at the base of the mixed layer continues to entrain iron from the layer that was previously in the mixed layer during winter. Hence, anticyclones have relatively iron-enriched water below the summertime mixed layer compared to cyclones (Figure 3a), and this may contribute to differences in iron limitation among the two types of features. This explanation can be applied to well-formed and long-lived eddies whose life spans are of the order of months. Given that many eddies along the ACC survive 3 months and longer (Frenger et al., 2015), the preconditioning explanation is plausible.

In other highly dynamic regions of intense eddy activity such as the Gulf Stream and the Kuroshio Current, it is thought that eddies cause anomalies of CHL concentration primarily through eddy-driven advection of large-scale CHL gradients, that is, stirring and trapping (Gaube et al., 2014; Kouketsu et al., 2015). The lateral gradient of CHL suggests that advective mechanisms cannot be entirely ruled out in understanding the correlations along the ACC (Figures S1c and S1d). However, the lateral gradient in CHL is not as strong as in either the Gulf Stream or the Kuroshio Current, owing to light limitation in the winter and iron limitation in the summer (the so-called High Nitrate Low Chlorophyll [HNLC] condition).

Understanding the influence of mesoscale processes on vertical mixing and iron supply is important for more accurate estimation of SO's role in global carbon cycle. However, coarse resolution climate modeling systems on which many studies rely do not resolve the ocean's mesoscale. Such models cannot capture mixed layer modulation by the mesoscale, leading to as yet unknown biases in air-sea carbon dioxide flux. Quantifying the integrated effects of these phenomena on biological uptake and the supply of carbon rich water from depth is necessary to better understand the role of the mesoscale in biogeochemical cycling in the SO.

Acknowledgments

The altimeter products were produced and distributed by AVISO (<http://www.aviso.altimetry.fr/>), as part of the Ssalto ground processing segment. The CHL observations are available through NASA MEaSUREs Ocean Color Product Evaluation Project (<ftp://ftp.oceancolor.ucsb.edu/>). The observational data for the depth of the mixed layer are from Dong et al. (2008) and for iron concentration are from Tagliabue et al. (2014). Computational facilities have been provided by the Climate Simulation Laboratory, which is managed by CISL at NCAR. NCAR is supported by the National Science Foundation. The CESM source code is freely available at <http://www2.cesm.ucar.edu>. The analysis code for the Fe budget averaged over the mixed layer is available at <https://github.com/hajsong/tracerbudget>. H. S., J. M., and D. J. M. were supported by the NSF MOBY project (OCE-1048926). D. J. M. also acknowledges support from NSF (OCE-1048897) and NASA (NNX13AE47G). In addition, P. G. acknowledges support from NSF (OCE-1558809) and NASA (NNX13AE47G and NNX16AH9G).

References

- Boyd, P. W. (2002). The role of iron in the biogeochemistry of the Southern Ocean and equatorial Pacific: A comparison of in situ iron enrichments. *Deep-Sea Research Part II*, 49(9–10), 1803–1821. [https://doi.org/10.1016/S0967-0645\(02\)00013-9](https://doi.org/10.1016/S0967-0645(02)00013-9)
- Boyd, P. W., & Ellwood, M. J. (2010). The biogeochemical cycle of iron in the ocean. *Nature Geoscience*, 3(10), 675–682.
- Carranza, M. M., & Gille, S. T. (2015). Southern Ocean wind-driven entrainment enhances satellite chlorophyll-a through the summer. *Journal of Geophysical Research: Oceans*, 120, 304–323. <https://doi.org/10.1002/2014JC010203>
- Carranza, M., Gille, S., Piola, A., Charo, M., & Romero, S. (2017). Wind modulation of upwelling at the shelf-break front off Patagonia: Observational evidence. *Journal of Geophysical Research: Oceans*, 122, 2401–2421. <https://doi.org/10.1002/2016JC012059>
- Chelton, D. B., Gaube, P., Schlax, M. G., Early, J. J., & Samelson, R. M. (2011). The influence of nonlinear mesoscale eddies on near-surface oceanic chlorophyll. *Science*, 334(6054), 328–332.
- Chelton, D. B., Schlax, M. G., & Samelson, R. M. (2011). Global observations of nonlinear mesoscale eddies. *Progress in Oceanography*, 91(2), 167–216. <https://doi.org/10.1016/j.pocean.2011.01.002>
- Clayton, S., Dutkiewicz, S., Jahn, O., Hill, C., Heimbach, P., & Follows, M. J. (2016). Biogeochemical versus ecological consequences of modeled ocean physics. *Biogeosciences Discussions*, 2016, 1–20. <https://doi.org/10.5194/bg-2016-337>
- Dong, S., Sprintall, J., Gille, S. T., & Talley, L. (2008). Southern Ocean mixed-layer depth from Argo float profiles. *Journal of Geophysical Research*, 113, C06013. <https://doi.org/10.1029/2006JC004051>
- Dufois, F., Hardman-Mountford, N. J., Greenwood, J., Richardson, A. J., Feng, M., Herbette, S., & Matear, R. (2014). Impact of eddies on surface chlorophyll in the South Indian Ocean. *Journal of Geophysical Research: Oceans*, 119, 8061–8077. <https://doi.org/10.1002/2014JC010164>
- Dufois, F., Hardman-Mountford, N. J., Greenwood, J., Richardson, A. J., Feng, M., & Matear, R. J. (2016). Anticyclonic eddies are more productive than cyclonic eddies in subtropical gyres because of winter mixing. *Science Advances*, 2(5), e1600282–e1600282.
- Fauchereau, N., Tagliabue, A., Bopp, L., & Monteiro, P. M. S. (2011). The response of phytoplankton biomass to transient mixing events in the Southern Ocean. *Geophysical Research Letters*, 38, L17601. <https://doi.org/10.1029/2011GL048498>
- Ferrari, R., & Wunsch, C. (2009). Ocean circulation kinetic energy: Reservoirs, sources, and sinks. *Annual Review of Fluid Mechanics*, 41, 253–282. <https://doi.org/10.1146/annurev.fluid.40.111406.102139>
- Frenger, I. (2013). On Southern Ocean eddies and their impacts on biology and the atmosphere (Ph.D. thesis) Zurich, Switzerland: ETH Zurich. <https://doi.org/10.3929/ethz-a-009938120>
- Frenger, I., Münnich, M., Gruber, N., & Knutti, R. (2015). Southern ocean eddy phenomenology. *Journal of Geophysical Research: Oceans*, 120, 7413–7449. <https://doi.org/10.1002/2015JC011047>
- Gaube, P., Chelton, D. B., Strutton, P. G., & Behrenfeld, M. J. (2013). Satellite observations of chlorophyll, phytoplankton biomass, and Ekman pumping in nonlinear mesoscale eddies. *Journal of Geophysical Research: Oceans*, 118, 6349–6370. <https://doi.org/10.1002/2013JC009027>
- Gaube, P., McGillicuddy, D. J., Jr., Chelton, D. B., Behrenfeld, M. J., & Strutton, P. G. (2014). Regional variations in the influence of mesoscale eddies on near-surface chlorophyll. *Journal of Geophysical Research: Oceans*, 119, 8195–8220. <https://doi.org/10.1002/2014JC010111>
- Hausmann, U., McGillicuddy, D. J., Jr., & Marshall, J. (2017). Observed mesoscale eddy signatures in Southern Ocean surface mixed-layer depth. *Journal of Geophysical Research: Oceans*, 122, 617–635. <https://doi.org/10.1002/2016JC012225>
- Kouketsu, S., Kaneko, H., Okunishi, T., Sasaoka, K., Itoh, S., Inoue, R., & Ueno, H. (2015). Mesoscale eddy effects on temporal variability of surface chlorophyll a in the Kuroshio Extension. *Journal of Physical Oceanography*, 72(3), 439–451.
- Large, W., McWilliams, J., & Doney, S. (1994). Oceanic vertical mixing: A review and a model with nonlocal boundary layer parameterization. *Reviews of Geophysics*, 32, 363–403.
- McGillicuddy, D. J., Jr. (2016). Mechanisms of physical-biological-biogeochemical interaction at the oceanic mesoscale. *Annual Review of Marine Science*, 8(1), 125–159.
- McGillicuddy, D. J., Jr., Anderson, L. A., Bates, N. R., Bibby, T., Buesseler, K., Carlson, C., et al. (2007). Eddy/wind interactions stimulate extraordinary mid-ocean plankton blooms. *Science*, 316, 1021–1026.
- Moore, J. K., Doney, S. C., Kleypas, J. A., Glover, D. M., & Fung, I. Y. (2002). An intermediate complexity marine ecosystem model for the global domain. *Deep-Sea Research Part II*, 49(1–3), 403–462.
- Moore, J. K., Doney, S. C., & Lindsay, K. (2004). Upper ocean ecosystem dynamics and iron cycling in a global three-dimensional model. *Global Biogeochemical Cycles*, 18, GB4028. <https://doi.org/10.1029/2004GB002220>
- Moore, J. K., Lindsay, K., Doney, S. C., Long, M. C., & Misumi, K. (2013). Marine ecosystem dynamics and biogeochemical cycling in the Community Earth System Model [CESM1(BGC)]: Comparison of the 1990s with the 2090s under the RCP4.5 and RCP8.5 scenarios. *Journal of Climate*, 26(23), 9291–9312. <https://doi.org/10.1175/JCLI-D-12-00566.1>
- Nelson, D. M., & Smith, W. O. (1991). Jr Sverdrup revisited: Critical depths, maximum chlorophyll levels, and the control of Southern Ocean productivity by the irradiance-mixing regime. *Limnology and Oceanography*, 36(8), 1650–1661.

- Robinson, A. R. (1983). *Eddies in Marine Science* (609 pp.). Berlin: Springer Verlag. <https://doi.org/10.1007/978-3-642-69003-7>
- Rodríguez, J., Tintoré, J., Allen, J. T., Blanco, J. M., Gomis, D., Reul, A., et al. (2001). Mesoscale vertical motion and the size structure of phytoplankton in the ocean. *Nature*, *410*(6826), 360–363.
- Tagliabue, A., Sallée, J.-B., Bowie, A. R., Lévy, M., Swart, S., & Boyd, P. W. (2014). Surface-water iron supplies in the Southern Ocean sustained by deep winter mixing. *Nature Geoscience*, *7*, 314–320. <https://doi.org/10.1038/ngeo2101>
- Venables, H., & Moore, C. (2010). Phytoplankton and light limitation in the Southern Ocean: Learning from high-nutrient, high-chlorophyll areas. *Journal of Geophysical Research*, *115*, C02015. <https://doi.org/10.1029/2009JC005361>
- Wunsch, C. (1999). Where do ocean eddy heat fluxes matter. *Journal of Geophysical Research*, *104*, 13,235–13,249.
- Xu, C., Shang, X.-D., & Huang, R. X. (2014). Horizontal eddy energy flux in the world oceans diagnosed from altimetry data. *Scientific Reports*, *4*, 5316. <https://doi.org/10.1038/srep05316>